Neuron, Vol. 21, 1031–1044, November, 1998, Copyright ©1998 by Cell Press

Pax6 Controls Radial Glia Differentiation in the Cerebral Cortex

Magdalena Götz,[‡§] Anastassia Stoykova,[*‡] and Peter Gruss[*†]
[*]Department of Molecular Cell Biology
Max-Planck Institute of Biophysical Chemistry
37077 Göttingen
Federal Republic of Germany

Summary

Radial glia cells perform a dual function in the developing nervous system as precursor cells and guides for migrating neurons. We show here that during forebrain neurogenesis, the transcription factor *Pax6* is specifically localized in radial glia cells of the cortex but not of the basal telencephalon. In *Pax6*-deficient mice, cortical radial glia cells were altered in their morphology, number, tenascin-C (TN-C) expression, and cell cycle. We show that some of these alterations are cell-autonomous, whereas others were rescued by coculturing with wild-type cortical cells. Our results suggest that *Pax6* plays an essential role in the differentiation of cortical radial glia. Thus, despite their widespread distribution, radial glia cells are regionally specified in the developing CNS.

Introduction

During neural development, precursor cells located in the ventricular and subventricular zone generate the distinct cell types of the adult brain. In the mammalian cerebral cortex, precursor cells are not a homogeneous population but consist of distinct subtypes (His, 1889; Gracheva, 1969; Levitt et al., 1981, 1983). More recently, cell lineage analysis has shown that distinct precursor pools in the cerebral cortex generate different sets of descendants in vivo and in vitro (Grove et al., 1993; Luskin et al., 1993; Reid et al., 1995; Williams and Price, 1995).

Despite the evidence for functional heterogeneity of cortical precursor cells, the only subset of precursor cells described at a cellular level are the radial glia cells. Radial glia is a prominent cell type in many regions of the vertebrate central nervous system (Ramón y Cajal, 1890; Misson et al., 1988; Edwards et al., 1990). Its cell somata reside in the VZ, with characteristic long radial processes that span the entire distance to the pial surface (Schmechel and Rakic, 1979b; Voigt, 1989). In the developing cortex, radial glia cells perform a dual role as precursor cells (Choi and Lapham, 1978; Levitt et al., 1983; Misson et al., 1991) and as migratory substrates for postmitotic neurons (Rakic, 1972; Gadisseux et al., 1990; Hatten and Mason, 1990). The correct specification of radial glia cells is therefore essential for normal organization of the developing cortex (e.g., see Pinto-Lord et al., 1982). Although a variety of molecules have been shown to be important for neuronal migration (Rakic et al., 1994), little is known about factors and mechanisms that specify the radial glia cells in the developing nervous system.

A first hint that the transcription factor *Pax6* might influence radial glia cells was obtained in our previous analysis of the boundary between the developing cortex and ganglionic eminence (GE) formed by radial glia cells. We observed that the prominent fasciculation of radial glia cells at this boundary fails to form in the *Pax6* mutant *Small eye* (Stoykova et al., 1997). In the absence of a functional Pax6 protein, several other abnormalities have been detected in the developing cortex: cytoarchitectonic alterations, failure of cell migration, and altered cell adhesion (Schmahl et al., 1993; Caric et al., 1997; Stoykova et al., 1997). It is not yet known, however, which of these defects are a direct consequence of the absence of Pax6 and which are secondary defects.

Here, we present evidence that the Pax6 protein is localized in a specific class of precursor cells, the radial glia. These cells are affected in the earliest stages of development in *Pax6* mutant mice (*Small eye* [*Sey*], Hill et al., 1991; *Pax6* −/−, St.-Onge et al., 1997). Radial glia cells are affected in their morphology, tenascin-C (TN-C) synthesis, and cell cycle characteristics. Moreover, we demonstrate that the morphological alterations of radial glia cells are cell-autonomous, suggesting an important role for Pax6 in the differentiation of cortical radial glia and thereby establishing regional differences between radial glia cells of other prospective brain regions e.g., the adjacent GE.

Results

Pax6 Protein Is Localized in RC2-Positive Subsets of Cortical Precursor Cells

The *Pax6* gene is known to be expressed in the VZ of the developing cortex (Walther and Gruss, 1991), but its cellular location has not yet been studied. To examine whether all precursor cells would contain the Pax6 protein, precursor cells were labeled by a 1 hr bromodeoxyuridine (BrdU) pulse (see Experimental Procedures), and sections of cortex at embryonic day 16.5 (E16.5) were double stained with a monoclonal antibody against BrdU and a polyclonal Pax6 antiserum. Since the BrdU pulse labels only cells in S phase, not all precursor cells are labeled. Interestingly, most but not all BrdU-immunoreactive nuclei (green) also contained the Pax6 protein (red) as depicted in Figure 1A. Notably, most of the double immunopositive cells were situated in the ventricular zone (VZ), whereas dividing cells that did not contain the Pax6 protein were more often localized some distance from the VZ. This colocalization demonstrates that some dividing cells do not contain Pax6 protein. Thus, Pax6 is only localized in a subpopulation of cortical precursor cells.

Since radial glia cells are known as a subpopulation

[†]To whom correspondence should be addressed (e-mail: pgruss@gwdg.de).
[‡]These authors contributed equally to this work.
[§]Present address: Max-Planck Institute of Neurobiology, 82152 Martinsried, Federal Republic of Germany

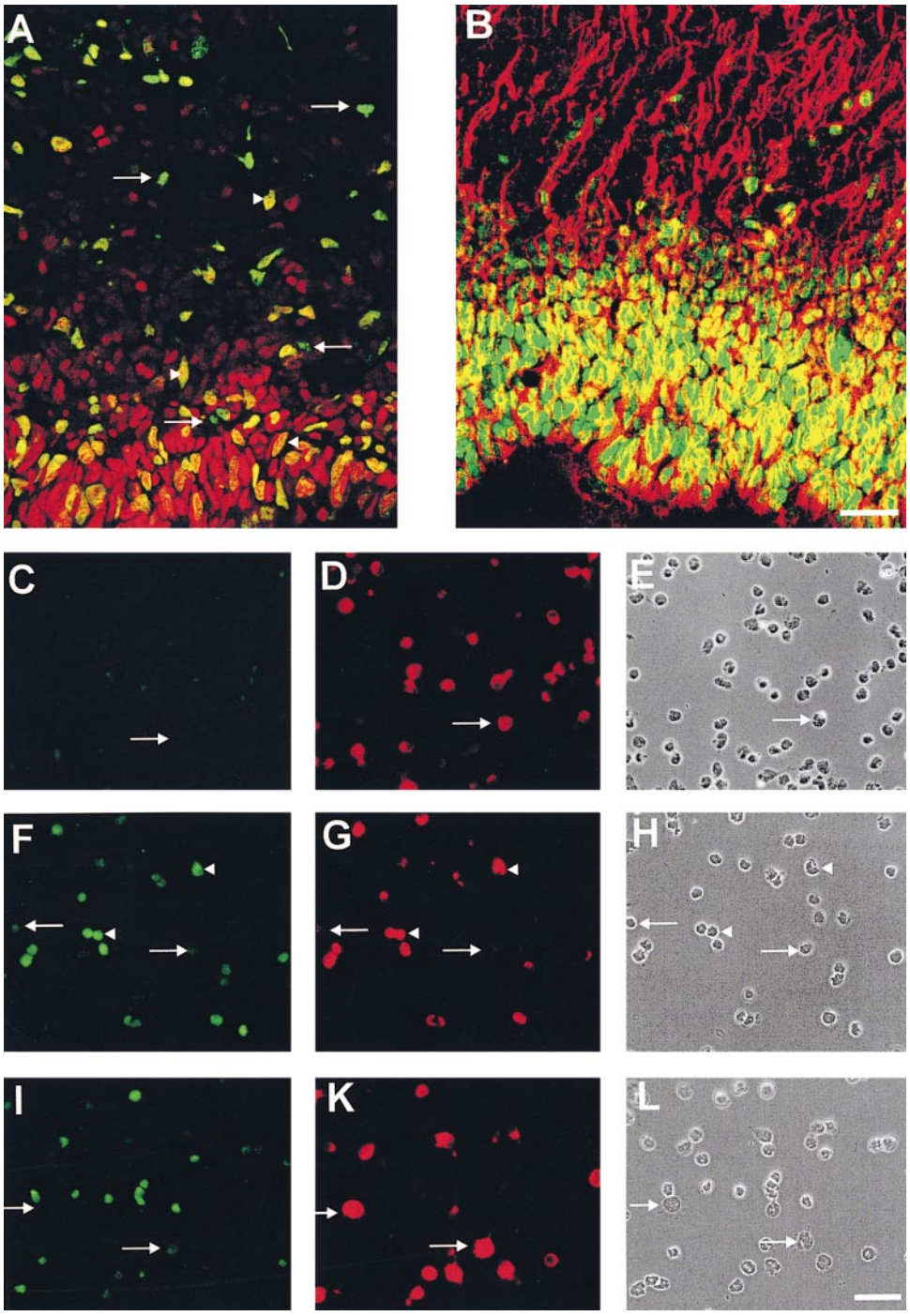

Figure 1. Radial Glia Cells from Cortex Are Pax6-Immunoreactive

(A) and (B) depict the ventricular side of a frontal section of an E16.5 cortex stained with Pax6- and BrdU-antiserum (A) or Pax6- and RC2-antiserum (B). BrdU was injected 1 hr prior to fixation.

(A) BrdU-labeled cells are green- and Pax6-labeled cells red-fluorescent. Examples of double labeled cells (appearing yellow) are indicated by arrowheads, and some cells labeled only with BrdU are marked by arrows. Note that not all BrdU-positive cells are also Pax6-positive, indicating that only a subpopulation of cortical precursor cells contains the Pax6 protein.

(B) Pax6-labeled cells appear in green and RC2-labeled processes in red. Note that most cells seem double labeled (yellow).

(C) through (E), (F) through (H), and (I) through (L) show corresponding phase (E, H, and L) and fluorescent (C, D, F, G, I, and K) micrographs of E13.5 acutely dissociated cells ([C] through [E] from E13.5 ganglionic eminence; [F] through [L] from cortex) stained with Pax6-antiserum (C, F, and I), the monoclonal antibody RC2 (D and G) and a monoclonal antibody directed against β-III-tubulin (K). Arrows indicate examples of single labeled cells, arrowheads depict cells that are double positive (F–H).

Note that RC2-immunoreactive cells from the cortex (G) are also Pax6-immunoreactive, whereas those from the ganglionic eminence are not (D and C). Cortical Pax6-positive cells are not β-III-tubulin-positive but RC2-positive, indicating that Pax6 labels cortical radial glia cells. Scale bar, 50 μm.

of precursor cells, we performed double label immunohistochemistry using anti-Pax6 and RC2, a monoclonal antibody that specifically labels radial glia cells (Edwards et al., 1990). As depicted in Figure 1B, most Pax6-immunoreactive nuclei (labeled in green) seem closely apposed to RC2-immunoreactive fibers (labeled in red) and thus appear yellow when double stained. Precise cellular colocalization in the sections, however, proved difficult, since RC2 immunoreactivity is found in processes, while Pax6 is localized in nuclei.

To perform a quantitative analysis of the cell types containing Pax6, we therefore turned to acutely dissociated cells from E13.5–17.5 cortex and GE. Double stainings combined the polyclonal Pax6 antiserum with the following monoclonal cell-type-specific antibodies: mAb RC2 to label radial glia cells, anti-nestin to label precursor cells, and anti-β-III-tubulin to detect neurons. Pax6-immunoreactive cells made up 49% (n = 1036) of all acutely dissociated cells from E13.5 cortex but only 5% (n = 958) of cells from the GE (Figures 1C–1E), consistent with the absence of Pax6 protein from this region in vivo. Pax6-immunoreactive cells were double labeled with anti-nestin (98%, n = 123) and RC2 (92%, n = 337) (Figures 1F–1H) but rarely with anti-β-III-tubulin (7%, n = 190) (Figures 1I–1L). This is consistent with the staining observed in vivo (Figures 1A and 1B), in which Pax6 is restricted to cortical precursor cells.

In agreement with previous studies (Edwards et al., 1990), RC2 also labels a subpopulation of precursor cells in acutely dissociated cells; all RC2-positive cells are also nestin-positive, but a subset of nestin-positive cells are RC2-negative. This is evident as well from the larger proportion of nestin-positive compared with RC2-positive cells of E13.5 cortical cells (see Figure 6). Interestingly, only the proportion of RC2-immunoreactive cells (56%) fits closely to the proportion of Pax6-positive cortical cells (49%). Indeed, almost all Pax6-positive cells were also RC2- (and nestin-) immunoreactive (92%, n = 337), and only a few Pax6-negative cells were stained with RC2 (17%, n = 304). In contrast, however, there was a considerably higher proportion of Pax6-negative cells that are nestin-positive (45%, n = 168). These results demonstrate that Pax6 is localized in a subpopulation of precursor cells that is mostly RC2- (and nestin-) positive. The precursor cells that do not contain Pax6 are mostly RC2-negative but nestin-positive.

The Pax6/RC2-positive subpopulation of the cortical precursors shows an intriguing developmental profile, since we noted a decrease of the overall proportion of RC2-positive cells (E13.5, 56%; E15.5, 24%). This is surprising in regard to the increased neuronal migration at later stages of neurogenesis. It was also surprising to see that RC2-immunoreactive cells made up such a large subpopulation of precursor cells (E13.5, 79%, n = 1205).

Taken together, the results from the in vivo and in vitro analysis show that the expression of the transcription factor *Pax6* is a prominent characteristic of radial glia cells in the developing cortex.

Radial Glia Morphology in *Pax6* Mutant Cortex

In Vivo Analysis

To address the function of *Pax6* mutants in radial glial, cells we analyzed the *Pax6* mutants *Small eye* (*Sey*, Hill et al., 1991) and *Pax6* −/− mice (St.-Onge et al., 1997). For all of the aspects described in the following, no differences between *Sey/Sey* and *Pax6* −/− mutants were observed (see Experimental Procedures), and we refer to both of these mutants as Pax6-deficient mice (Pax6-def).

First, we labeled radial glia cells with 1,1′-dioctadecyl-3,3,3′,3′-tetramethylindocarbocyanine (DiI) from the pial side as described by Voigt (1989). As depicted in Figure 2A, radial glia cells in the cortex of E15.5 wild-type mice have rather straight processes running toward the pial surface. In contrast, DiI-labeled cortical radial glia cells in corresponding sections of the cortex of *Pax6* mutant littermates appear wavy in comparison to the wild-type. Examples of very sharp turns of the radial glia fibers are easily detectable in the *Pax6* mutant cortex (Figure 2B) but not in the wild-type cortex. In addition, Pax6-deficient radial glia exhibits frequent small extrusions and branches. These morphological differences were observed from the ventricular to the pial surface (Figures 2A and 2B).

Morphological alterations of radial glia cells were also observed after RC2 immunostaining. As depicted in Figures 2C and 2D, RC2-labeled processes run straight through the cortical plate in wild type, whereas in the Pax6-deficient cortex, plenty of small labeled processes running in parallel to the pial surface could be observed. As described by Caric et al. (1997), we also observed prominent fasciculation of RC2-positive processes in the intermediate zone in the *Pax6* mutant cortex (Figure 2D). Thus, both labeling techniques revealed alterations in the morphology of radial glia cells in the cortex of *Pax6* mutant mice.

In Vitro Analysis

The morphological defects of *Pax6* mutant cortical radial glia cells could be a consequence of morphogenetic changes, since the cortical plate in the *Sey* brain is smaller and thinner than normal (Schmahl et al., 1993). We therefore analyzed RC2-labeled cells in dissociated cell cultures, where morphogenetic differences should play no role. Indeed, we detected prominent morphological differences between RC2-positive cells from E13.5 wild-type and Pax6-deficient cortex in dissociated cell culture after 2 days in vitro. Whereas many RC2-positive cells from wild-type cortex exhibited a bipolar morphology (Figure 3A; see also Culican et al., 1990; Hunter and Hatten, 1995), most RC2-positive cells from Pax6-deficient cortex had short processes and a multipolar morphology (Figure 3C; for quantitation, see Table 1). Thus, the morphological alterations of Pax6-deficient cortical radial glia are independent of morphogenetic alterations in vivo.

Interestingly, RC2-positive cells in cultures from wild-type GE also exhibited a different morphology than the one observed in wild-type cortical cultures (Figures 3A and 3B). This difference is quite prominent, since 66% of the cortical RC2-positive cells possess processes longer than their soma (n = 101), while only 31% (n = 139) of the cells from the wild-type GE have this characteristic. Thus, RC2-positive cells from distinct domains of wild-type telencephalon differ in their morphology in vitro, indicating intrinsic regional differences of radial glia cells. Also noteworthy, the morphology of RC2 cells from *Pax6* mutant cortex apparently resembles the one

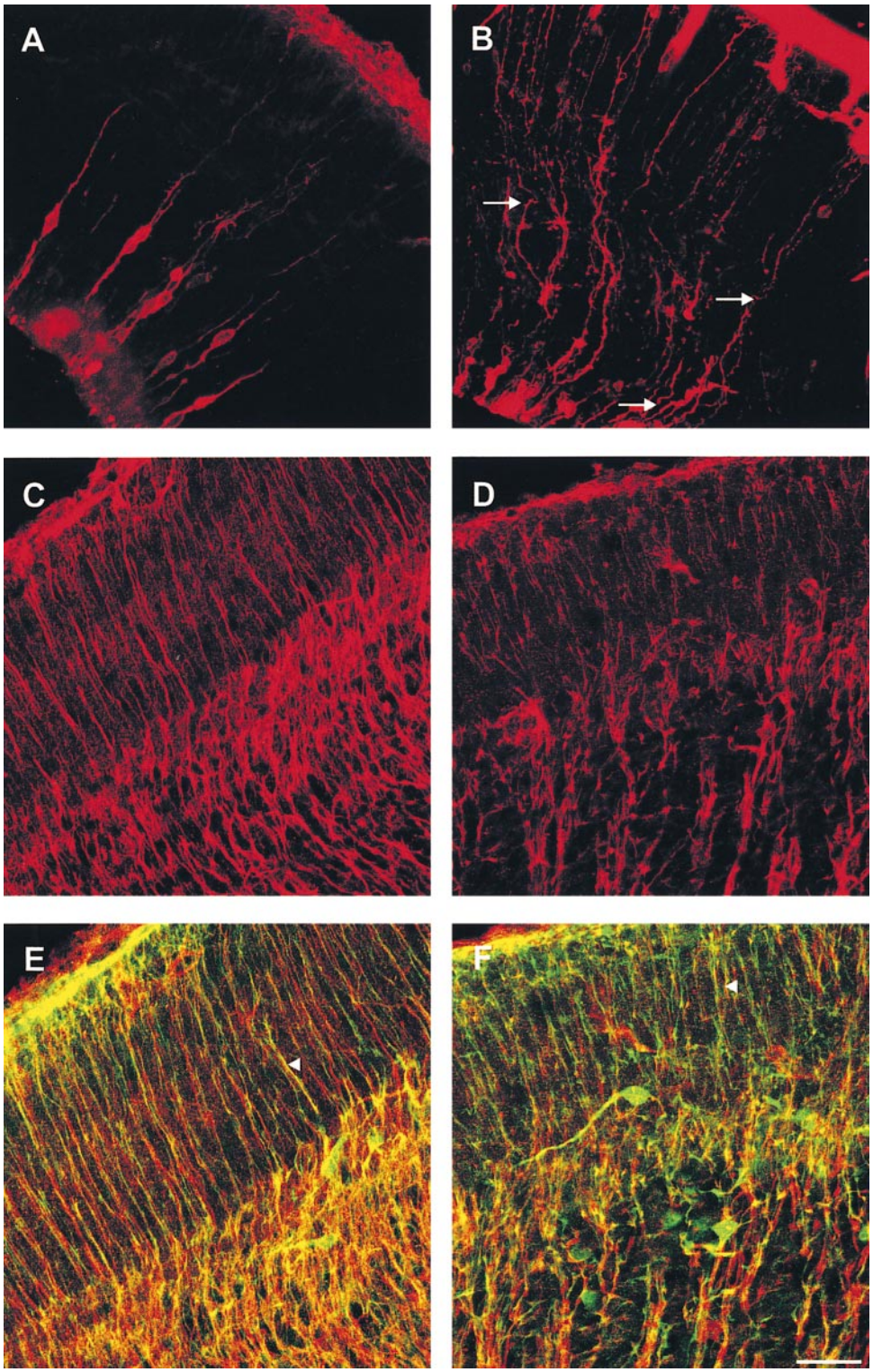

Figure 2. Altered Morphology of Radial Glia Cells in *Pax6* Mutant Cortex in Vivo

Fluorescent micrographs of corresponding sections from E15.5 (A and B) and E16.5 (C–F) wild-type (A, C, and E) and *Pax6* mutant (B, D, and F) cortex cut frontally. Vibratome sections are 100 μm thick, and several optical sections are shown in (A) and (B) (8) and (E) and (F) (2), whereas (C) and (D) depict a single opic section. All micrographs are orientated with the pial side up (upper right corner in [A] and [B]; upper left corner in [C] through [F]).

(A) and (B) show radial glia cells labeled with DiI from the pial surface. Note the sharp bends in radial glia processes in the *Pax6* mutant cortex indicated by arrows in (B) that are not visible in the wild-type.

Sections in (C) through (F) have been double stained with the monoclonal antibody RC2 (red) and polyclonal antiserum against BLBP (green) to label radial glia cells.

(C) and (D) depict RC2-labeled processes in a single optical section. Note the disorganization of fibers in the *Pax6* mutant (D) in comparison to the wild-type cortex (C).

(E) and (F) show RC2 (red) and BLBP (green) immunoreactivity, and examples of double labeled processes are indicated by an arrowhead. Some horizontally orientated BLBP-immunoreactive cells are also stained in both the wild-type and the mutant cortex. Note the comparable BLBP immunoreactivity in the *Pax6* mutant (F) and wild-type (E) cortex despite the morphological differences. Scale bar, 25 μm.

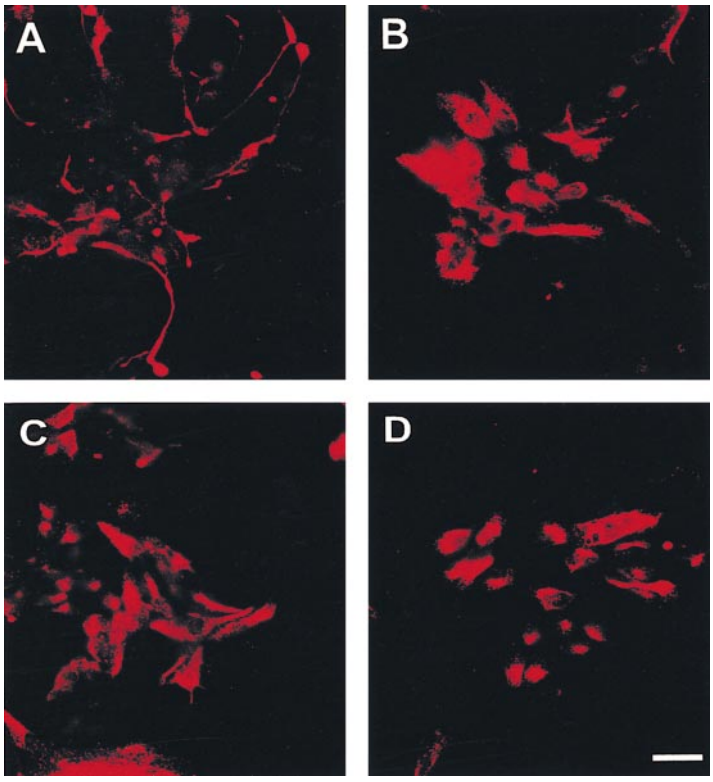

Figure 3. Altered Morphology of Radial Glia Cells of *Pax6* Mutant Cortex in Vitro

Fluorescent micrograph of RC2-immunoreactive cells from E14.5 wild-type cortex (A), ganglionic eminence (B), *Pax6* mutant cortex (C), and ganglionic eminence (D) after 2 days in vitro. Note that RC2-positive radial glia from wild-type cortex exhibit a bipolar morphology distinct from those of *Pax6* mutant cortex. Interestingly, radial glia cells of the ganglionic eminence have a different morphology than those from the cortex (B and D). Scale bar, 25 μm.

observed in GE cultures (compare Figure 3C with Figures 3B and 3D). This strongly suggests that *Pax6* is involved in the regional patterning of radial glia in the developing telencephalon.

Expression of Radial Glia–Specific Markers

To exclude the possibility that the RC2-positive cells in the *Pax6* mutant assume a different phenotype while only maintaining RC2 expression, we used additional markers for radial glia cells. Brain lipid–binding protein (BLBP) and GLAST have been described to be expressed by radial glia cells even though they also label other cell populations (Feng et al., 1994; Kurtz et al., 1994; Shibata et al., 1997). BLBP is of particular interest in this regard, since it is known to be induced by neurons attaching to and migrating along radial glia fibers (Feng et al., 1994). Interestingly, BLBP-immunoreactive processes were present in *Pax6* mutant cortex and also colocalized with RC2 labeling as in the wild-type cortex (Figures 2E and 2F). Again, we used acutely dissociated cells to quantitate the number of BLBP-immunoreactive cells and found no difference between the wild-type and Pax6-deficient cortex (E16.5, wild-type cortex, 26%, n = 276; Pax6-def cortex, 25%, n = 309). This aspect of radial glia phenotype therefore seems unaffected in the *Pax6* mutant cortex.

To further analyze the phenotype of radial glia cells in the *Pax6*-deficient mice, we examined the expression of the extracellular matrix (ECM) molecule TN-C, which has been previously localized in radial glia cells (Bartsch et al., 1992). In the VZ of telencephalon, TN-C is strongly expressed at E14.5, most prominently at the corticostriatal sulcus (Figure 4A and Götz et al., 1997). Interestingly, in Pax6-deficient mice, this expression is lost in the cortical VZ (where *Pax6* is normally strongly expressed), while the expression in the neuroepithelium of the GE is still present even though it appears reduced (Figure 4B). At later stages, however, when gliogenesis takes over in the cortex (E18.5), scattered TN-C-synthesizing cells appeared throughout the *Pax6*-deficient cortex as in the wild-type cortex (Figures 4D and 4F). Such cells have been double stained with glia fibrillary acid protein (GFAP) and hence have been identified as astrocyte precursors (Mitrovic et al., 1994). Thus, TN-C synthesis is mainly disturbed during neurogenesis in the VZ of *Pax6* mutant cortex.

Table 1. Coculture Analysis of Radial Glia Cell Morphology

Cultured Cells	Percentage of RC2+ Cells with Long Processes
E13.5 *Pax6* −/− cortex	100%
E13.5 wild-type cortex	204% (± 18%)
E13.5 *Pax6* −/− cortex + 10× *Pax6* −/− cortex	100%
E13.5 *Pax6* −/− cortex + 10× wild-type cortex	93% (± 8%)

Morphological analysis. E13.5 *Pax6* −/− and wild-type cortical cells were cultured for 1–2 days on their own (first two rows from the top), and the proportion of RC2-positive cells with at least one long process (defined as exceeding the cell soma size) was assessed. Data were normalized to the proportion observed in *Pax6* −/− cultures. The number of cells analyzed from the top is n = 336, n = 341, n = 65, and n = 676. Note that the wild-type cortex contains more RC2-positive cells with long processes (204%) compared with the *Pax6* −/− cortex. No change in this parameter was achieved by coculturing with a 10× excess of wild-type cortical cells.

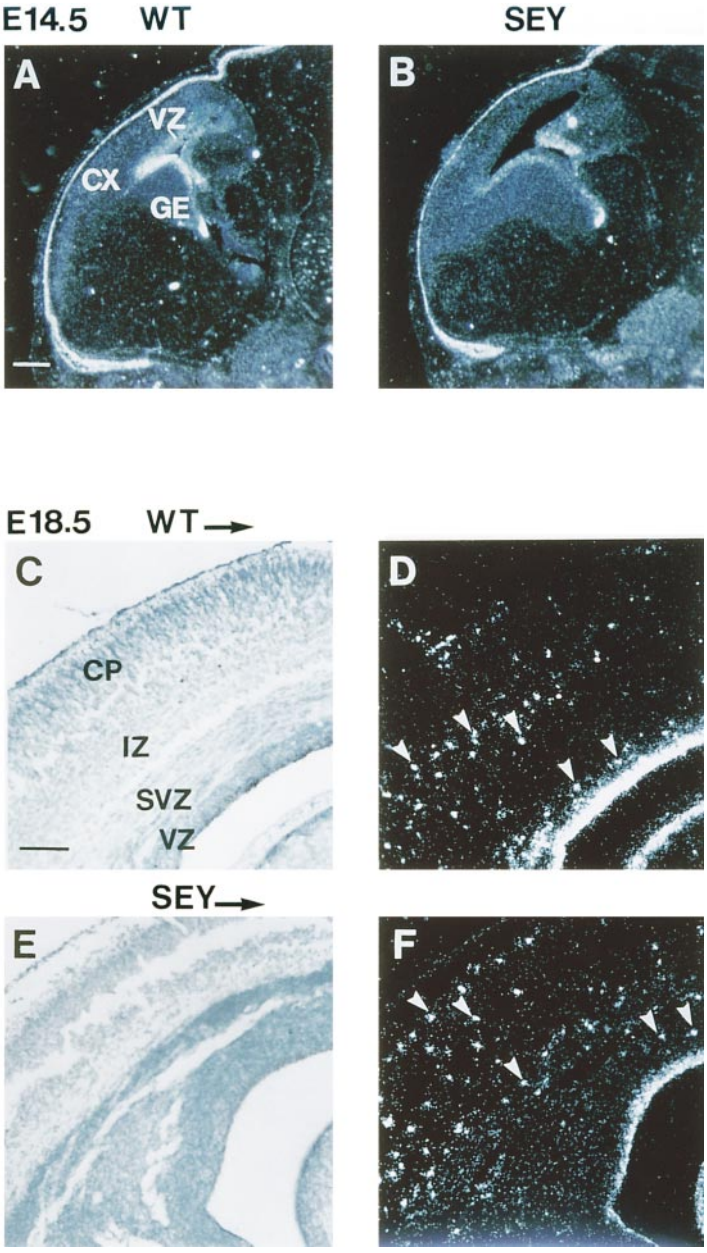

Figure 4. Deficit of TN-C Synthesis in *Pax6* Mutant Cortex

Sagittal sections of E14.5 (A and B) and coronal sections of E18.5 (C–F) wild-type (A, C, and D) or *Pax6* mutant (B, D, and F) cortex hybridized with a TN-C anti-sense RNA probe. (C), (D), (E), and (F) show corresponding phase contrast and dark field micrographs. Note that the TN-C synthesis is strongly impaired in the VZ of *Pax6* mutant cortex at E14.5 but occurs normally at later stages in cells scattered through the cortex (arrowheads in [D] and [F]). Scale bars, 200 μm (A and B); 150 μm (C–F).

Taken together, these results indicate that cortical radial glia cells exhibit specific defects in their differentiation program in the absence of functional *Pax6*, since they express some markers normally but are deficient in other aspects such as their morphology and TN-C synthesis.

Cell Cycle Deficit in the *Pax6* Mutant Cortex

To examine possible alterations in the mitotic cycle of the mutant cortical cells, we performed in vivo BrdU pulse labeling of wild-type and mutant embryos (see Experimental Procedures). After an hour, BrdU pulse cells in S phase are labeled, and after 6 hr, the BrdU injection–labeled cells progressed into M phase. During S phase, most nuclei are located some distance from the ventricular surface (Figure 5A, 1 hr BrdU pulse); they then move toward it during M phase (Figure 5C, 6 hr BrdU pulse), a phenomenon called interkinetic nuclear migration (Sauer, 1935). This differential location was not detectable in the *Pax6* mutant cortex, where BrdU labeled cells appeared scattered at similar positions after a 1 or 6 hr BrdU pulse (Figures 5B and 5D). This finding could either be due to a failure of interkinetic nuclear migration or to asynchronous cycling of precursor cells in the mutant cortex. In addition to alterations in the position of BrdU-labeled cells in *Pax6* mutant cortex, the number of BrdU-positive nuclei seemed to be increased in comparison to wild-type littermates (Figure 5). This difference was observed between E13.5–16.5 and decreased thereafter until it was not detectable at E18.5 (data not shown). Thus, the alterations in BrdU labeling in the *Pax6*-deficient cortex were restricted to

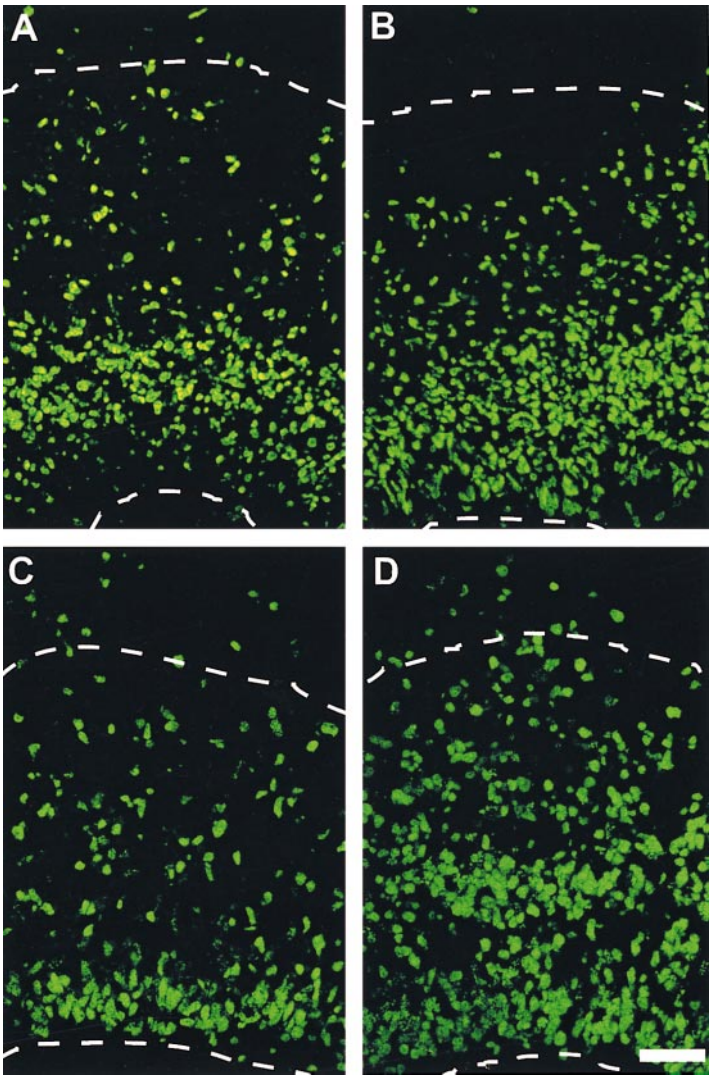

Figure 5. BrdU-Labeled Cells in Wild-Type and *Pax6* Mutant Cortex

BrdU pulse–labeled cells after a 1 hr (A and B) or 6 hr pulse (C and D) in transverse sections of E16.5 wild-type (A and C) and *Pax6* mutant (B and D) cortex. The VZ is delineated by the white dashed line (ventricular surface at the bottom). Note the increase in BrdU pulse–labeled cells in *Pax6* mutant cortex. In addition, the distribution of labeled nuclei differs between wild-type (A and C) and *Pax6* mutant (B and D) cortex. Scale bar, 50 μm (C and D).

the period of neurogenesis and disappeared when gliogenesis started.

The increased number of BrdU pulse–labeled cells in the *Pax6* mutant cortex could be explained either by an increase in the precursor cell population (predicting a higher number of nestin/proliferating cell nuclear antigen– [PCNA-] positive cells in *Pax6* mutant cortex) or an alteration in cell cycle properties (predicting a higher labeling index, LI = proportion of cycling cells in S phase). We tested these two possibilities by quantitative analysis of cell types and the LI again using acutely dissociated cell preparation. Figures 6A and 6B depict the quantitative analysis of cell types and BrdU-labeled cells in wild-type (gray bars) and *Pax6* mutant (white bars) cortex (A) and GE (B). Interestingly, there is no difference in the number of precursor cells (labeled by nestin or PCNA) between the wild-type and the *Pax6* mutant cortex at E13.5 ($p = 0.07$; Figure 6A). This indicates that the total proportion of precursor cells is not affected in the *Pax6* mutant cortex. However, their composition was altered; we observed a significant increase in the number of RC2-positive cells in the *Pax6* mutant cortex compared with the wild-type cortex (Figure 6A; $p = 0.0005$). Thus, in the *Pax6* mutant cortex, at E13.5 all precursor cells are RC2-immunoreactive, and the nestin-positive/RC2-negative population evident in the wild-type cortex (see above and Figure 6A) is lost in the absence of Pax6. This difference was not observed in the GE.

Consistent with the BrdU labeling in vivo, we also observed a significant increase in the number of BrdU pulse–labeled cells in acutely dissociated preparations from wild-type to *Pax6* mutant cortex (Figure 6A; $p = 0.001$). Thus, the proportion of BrdU pulse–labeled precursor cells, the labeling index (LI) differs between cells from wild-type (30%) and Pax6-deficient cortex (45%). This difference disappeared when gliogenesis started (LI E17.5, 32%, wild-type cortex; 39%, Pax6-def cortex). Since the LI gives an indication of cell cycle parameters, these data show that the cell cycle properties of cortical cells are affected in the absence of Pax6. These defects were not apparent in the GE (Figure 6B) and seem to be restricted to the period of neurogenesis in the *Pax6* mutant cortex.

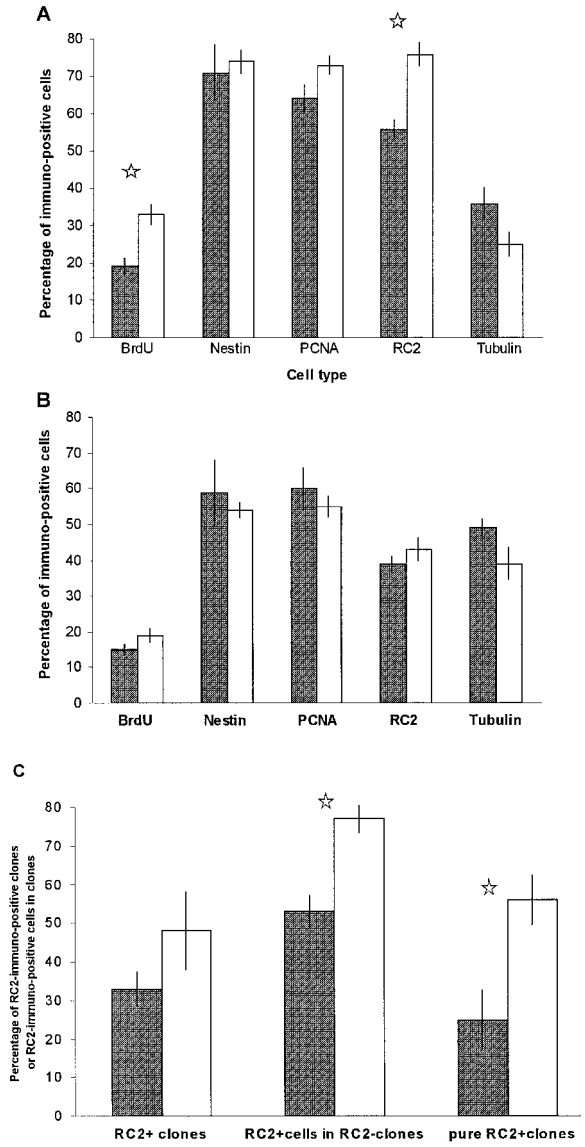

Figure 6. Quantitative Analysis of Cell Types in the Cortex of E13.5 Wild-Type and *Pax6* Mutant Mice

In all histograms, the y-axis depicts the percentage of cells (A and B) or the percentage of clones (C). Significant differences (Mann-Whitney U test, $p < 0.01$) between wild-type and Pax6 mutants are indicated by a star.

The cells analyzed in (A) and (B) were acutely dissociated (2 hr in vitro). The cells in (C) were cultured for 2 days in vitro.

The histogram in (A) depicts the percentage of cell types as indicated in the graph from E13.5 wild-type (gray bars) and *Pax6* mutant (white bars) cortex. BrdU pulse labeling was performed for 2 hr. The number of cells analyzed are (from left to right) wild-type cortex, n = 1400, n = 602, n = 1205, n = 971, n = 602; and Pax6-def cortex, n = 1473, n = 540, n = 2201, n = 768, n = 467. Note the significant increase in the number of BrdU pulse and RC2-labeled cells in *Pax6* mutants in comparison to wild-type littermates, while the overall number of precursor cells (nestin/PCNA-positive) is not altered.

The histogram in (B) depicts the percentage of cell types as indicated in the graph from E13.5 wild-type (gray bars) and *Pax6* mutant (white bars) ganglionic eminence. The number of cells analyzed are (from left to right) wild-type striatum, n = 401, n = 216, n = 475, n = 1513, n = 716; and Pax6-def striatum, n = 1236, n = 485, n = 628, n = 1332, n = 795. No significant differences in the frequency of any cell type could be detected between *Pax6* mutant and wild-type ganglionic eminence, consistent with the absence of *Pax6* expression in this region in wild-type animals.

The histogram in (C) depicts the clonal analysis of RC2-labeled cells in 2-day-old cultures from E13.5 wild-type (gray bars) and *Pax6* mutant (white bars) cortex. The two left bars depict the percentage of clones containing RC2-immunoreactive cells. The two bars in the center depict the percentage of RC2-positive cells in clones that contain RC2-positive cells. The two right bars depict the percentage of RC2-positive clones that contain only RC2-positive cells i.e., pure RC2 clones. Note the significant increase in the number of RC2-positive cells per clone in the *Pax6* mutant cortex.

The increased number of RC2-positive cells in *Pax6* mutant cortex, however, might affect the overall LI of precursor cells. Therefore, we directly compared the LI of RC2-positive cells in E13.5 wild-type (34%, n = 260) and the Pax6-deficient cortex (52%, n = 215). This difference indicates that RC2-positive cells in the cortex have different cell cycle properties in the absence of functional Pax6. Again, this difference was not observed in the GE, where the LI of RC2-positive cells was similar between wild-type (45%, n = 174) and *Pax6* mutant littermates (45%, n = 177). Thus, in the absence of functional Pax6, the cell cycle kinetics of cortical RC2-positive cells is altered.

Altered Composition of the Radial Glia Cell Lineage

As described above, we observed a significant increase in the number of RC2-positive cells in the *Pax6* mutant cortex compared with the wild-type cortex at E13.5. This persists throughout neurogenesis (percentage of RC2-positive cells in *Pax6* −/− versus wild-type: at E13.5, 136%; at E15.5, 121%; at E17.5, 160%) even though the absolute proportion of RC2-labeled cells decreases in the *Pax6* mutant cortex in parallel to the decrease in the wild-type. Thus, the transformation of the RC2-positive cells seems to occur normally in the absence of functional Pax6 despite the increased number of RC2-labeled cells in the mutant throughout neurogenesis. This increase could be explained by alterations in either cell death or cell lineage.

First, we performed a TdT-mediated dUTP nick ending labeling (TUNEL) staining of E13.5 wild-type and Pax6-deficient forebrain to evaluate the amount of cell death in *Pax6* mutant versus wild-type cortex. A very similar picture of apoptotic cells was seen in the wild-type and *Pax6* mutant cortex and GE; double staining with TUNEL and RC2 immunohistochemistry also revealed no differences. Thus, the increase in the number of RC2-positive cells cannot be explained by a reduction in cell death.

In contrast, significant alterations in the composition of clones containing RC2-positive cells were observed between wild-type (gray bars) and *Pax6* mutant (white bars) cortical cells (Figure 6C). Cortical cultures were infected at the day of plating with a low titre of the retroviral vector BAG (see Experimental Procedures), and β-galactosidase/RC2-double staining was performed after 2 days. In wild-type cortical cultures, 33% of all clones (n = 170) were RC2-positive, in contrast to 45% in Pax6-deficient cortical cultures (n = 113). Thus, there is an overall increase in the precursor cells that generate radial glia cells, but this difference is not statistically significant (Mann-Whitney U test, p = 0.05). A significant

difference was found, however, when we analyzed the number of RC2-positive cells per clone. As described above, all RC2-positive cells in a clone were also nestin-positive, but in cultures from wild-type cortex, some nestin-positive cells were RC2-negative. In addition, 48% of the clones of RC2-cells also contained tubulin-positive (RC2-negative) cells. Thus, in cultures from wild-type cortex, most clones containing RC2-positive cells also contained other cell types, and only 25% of these clones were composed exclusively of RC2-positive cells i.e., "pure" clones. Similar results have been obtained in vivo for the mammalian GE and chick tectum (Gray and Sanes, 1992; Halliday and Cepko, 1992). In contrast, in cortical cultures of *Pax6* mutant littermates, 55% of the clones containing RC2-positive cells were pure. This is a significant difference (Mann-Whitney U test, $p = 0.006$) that is also reflected in a significant increase in the overall percentage of RC2-labeled cells in the RC2-positive clones (53% in wild-type, 77% in *Pax6* mutant cortex, $p = 0.003$). These results show that individual precursor cells generate more radial glia cells in the absence of functional Pax6.

In contrast to the number of RC2-positive cells generated, the size of the clones was not affected. The mean size of all clones is 2.5 ($n = 335$) for the wild-type cortex and 2.6 ($n = 244$) for the Pax6-deficient cortex. Interestingly, the size of the clones that contain RC2-positive cells is larger, but is still the same for the wild-type (3.8, $n = 170$) and the Pax6-deficient cortex (3.8, $n = 113$). The mean clonal sizes of 2.5 and 3.8, respectively, suggest that most cells undergo only 1–2 cell cycles during the 2 days in vitro ($\log_2 2.5 = 1.3$; $\log_2 3.8 = 1.9$). This number of cell divisions is most likely too small to detect alterations in cell cycle length that should build up through several cell cycles to achieve changes in the number of cells generated. It should be possible, however, to detect alterations in the number of symmetric and asymmetric cell divisions. We therefore think that the mode of division is not altered in the *Pax6* mutant cortex, since the clonal size is not changed.

Diffusible Factor Regulates the Number but Not the Morphological Phenotype of Cortical Radial Glia

Two changes were observed in the cortex of the *Pax6* mutant: defects in the phenotype of RC2-positive cells and their higher number. Whereas the first is consistent with the specific localization of Pax6 in the radial glial cells and could suggest a direct influence of Pax6 on radial glia differentiation, the second finding is somewhat surprising and could be explained by indirect mechanisms involving cell–cell signaling. To directly test the latter hypothesis, we cocultured E13.5 Pax6-deficient cortical cells with a 10× excess of fluorescently labeled cells from the wild-type cortex (and for control with 10× *Pax6*-deficient cortical cells). We analyzed both the morphology and the number of RC2-positive cells in cocultures after 1–2 days in vitro.

The proportion of RC2-positive cells with processes longer than the cell soma was twice as high in cultures from wild-type cortex compared with *Pax6* mutant cortex (Table 1). This parameter was not affected when the *Pax6*-deficient cortical cells were cocultured with 10× cells from wild-type cortex (Table 1). These results strongly suggest that the morphological alterations of radial glia cells in the mutant cortex are cell-autonomous, since they cannot be rescued by coculturing with wild-type tissue.

Table 2. Coculture Analysis of the Proportion of Radial Glia Cells

Cultured Cells	Percentage of RC2+ Cells
E13.5 *Pax6* −/− cortex	100%
E13.5 wild-type cortex	61% (±5%)
E13.5 *Pax6* −/− cortex + 10× *Pax6* −/− cortex	100%
E13.5 *Pax6* −/− cortex + 10× wild-type cortex	65% (±8%)
E13.5 *Pax6* −/− cortex + 10× *Pax6* −/− cortex on filter	100%
E13.5 *Pax6* −/− cortex + 10× wild-type cortex on filter	68% (±5%)

Frequency analysis. E13.5 *Pax6* −/− and wild-type cortical cells were cultured for 1–2 days on their own (first two rows from the top), and the proportion of RC2-positive cells of all phase bright cells was analyzed and normalized to the proportion observed in *Pax6* −/− cultures. The number of cells analyzed from the top is $n = 1574$, $n = 1492$, $n = 229$, $n = 237$, $n = 704$, and $n = 1676$. Note that there are fewer (61%) RC2-positive cells in wild-type cortical cultures. The relatively high proportion of RC2-labeled cells in *Pax6* −/− cortical cultures was significantly reduced (Mann-Whitney U-test, $p < 0.01$) when cocultured with a 5–10× excess of wild-type cortical cells but not with *Pax6* −/− cells. Note that this reduction in the number of RC2-positive cells in *Pax6* −/− cortex achieves almost the level observed in the wild-type cortex. The same effect was observed when wild-type cells were cultured on a filter membrane (pore size, 3 μm).

In contrast, the number of RC2-positive cells was influenced in cocultures with 10× wild-type cortical cells. In single cultures of E13.5 wild-type cortical cells, the proportion of RC2-positive cells was 39% lower than in *Pax6*-deficient cortical cultures (Table 2). *Pax6*-deficient cortical cells cocultured with the 10× wild-type cortex reduced the proportion of RC2-immunoreactive cells by 35% compared with cocultures with 10× *Pax6* mutant cortical cells (Table 2). Thus, the difference in the number of RC2-positive cells between *Pax6* mutant and wild-type was almost abolished when *Pax6* mutant cells were cocultured with the wild-type cortex. To determine whether this effect requires direct cell–cell contacts, we cultured the wild-type cells on filter membranes (3 μm pore size). Even under these conditions, cocultures with 5 or 10× wild-type cortical cells lead to a significant decrease in the number of RC2-positive cells (Table 2; $p = 0.002$). Thus, a diffusible factor regulates the number of RC2-positive cells, consistent with previous observations by Hunter and Hatten (1995). This factor seems to be absent in the *Pax6* mutant cortex.

Discussion

In this study, we have shown that Pax6 is specifically localized in RC2-positive cortical cells during neurogenesis, and several aspects of these cells are affected in the absence of *Pax6* function. Most of the observed defects were restricted to the cortex and did not occur in the adjacent GE of *Pax6* mutants, an area where *Pax6*

is not expressed. Thus, *Pax6* plays an important role in the differentiation of cortical radial glia cells and thereby seems to generate differences between radial glia cells located in the cortex and the adjacent GE.

Validity of Markers

Radial glia cells exhibit ultrastructural criteria similar to glial cells such as bundles of filaments and glycogen accumulation (Rakic, 1972). Radial glia cells contain nestin as other precursor cells (Hockfield and McKay, 1985) and express some glial markers e.g., GFAP (only in primates) (Bignami and Dahl, 1974; Levitt et al., 1981), vimentin (Pixley and DeVellis, 1984), or the astrocyte-specific glutamate transporter GLAST (Shibata et al., 1997). Moreover, at the end of neurogenesis and neuronal migration, radial glia cells seem to transform into astrocytes in some CNS regions e.g., the cerebral cortex but not in others e.g., the cerebellum (Pixley and DeVellis, 1984; Voigt, 1989).

Radial glia cells and astrocytes are stained by the RC1 antibody (Edwards et al., 1990). In contrast, RC2 immunoreactivity is found to be restricted to the radial glia cells; it stains a subpopulation of precursor cells, and after neuronal migration, it disappears when radial glia transforms into astrocytes or more mature cell types such as Bergmann glia (Misson et al., 1988). BLBP labels only a subpopulation of radial glia cells as well as some neurons (Kurtz et al., 1994). Therefore, RC2 has been widely accepted as the best radial glia marker (Hunter and Hatten, 1995; Soriano et al., 1997).

It is not yet clear, however, to what extent the different antigens present on radial glia cells (RC2/GLAST/BLBP) colocalize. In our double staining with BLBP- and RC2-antibody, we observed both double labeled as well as single labeled processes, suggesting that there might be more heterogeneity in the radial glia population than previously assumed (E. Hartfuss and M. G., unpublished data). In light of the decrease in RC2-positive cells during the neurogenesis observed in this study, it will be important to analyze the developmental profile of these different markers. It is conceivable that radial glia cells change the expression of some of these markers during differentiation.

Pax6 and Radial Glia Cell Differentiation

The combination of different markers in this analysis (such as the morphology by DiI labeling and BLBP, GLAST, RC2, and nestin immunoreactivity) ensures that the cell types that express Pax6 and exhibit the defects in *Pax6* loss-of-function are radial glia cells. In the absence of functional Pax6, cortical radial glia cells exhibit an alteration in their morphology, number, and cell cycle kinetic. They are deficient in TN-C expression but still express BLBP, GLAST, and nestin. The restriction of these defects to the region of formerly normal *Pax6* expression supports the conclusion that it is the absence of functional Pax6 protein that distorts some aspects of the differentiation of cortical radial glia cells.

This phenotype might explain the previously reported defects in neuronal migration in the *Pax6* mutant cortex. An enlarged ventricular/subventricular zone of the cortex, cortical heterotopias, and a thin cortical plate have been observed in the cortex of *Sey* mutant mice (Schmahl et al., 1993). Evidence from BrdU labeling experiments revealed defects in neuronal migration (Caric et al., 1997; M. G., A. S., and P. G., unpublished data). These defects were mostly detected during later stages of neurogenesis, when migration depends upon radial glia cells, and were less obvious during earlier stages, when neurons migrate without radial glia guides (see also Stoykova et al., 1997). These observations are consistent with the notion that the defects in radial glia cells might be primarily responsible for the migrational aberrations in *Pax6* mutant cortex.

Since, however, glia-guided migration requires an especially tight interplay between radial glia and migrating neurons, it is difficult to assess whether neuronal defects might also contribute to the failure of migration in the *Pax6* mutants. Transplantation experiments demonstrated that neurons derived from *Pax6* mutant precursor cells migrate normally in a wild-type environment (Caric et al., 1997). This indicates that cortical neurons of *Pax6* mutant mice are either normal in this aspect or that their defects can be rescued in a wild-type environment. Normal neuron-to-glia signaling in the absence of *Pax6* is demonstrated by the normal expression of BLBP. BLBP is induced in radial glia cells by neurons attaching or migrating along them (Feng et al., 1994; Feng and Heintz, 1995). Thus, despite altered migration in the *Pax6* mutant cortex, these neurons induce BLBP in *Pax6* mutant radial glia cells.

BLBP was also shown to mediate the elongation of radial glia cells induced by the release of glial growth factors (GGFs) by the cortical migrating neurons (Anton et al., 1997). This elongated morphology of radial glia cells, however, is severly distorted in *Pax6* mutant radial glia cells despite the presence of BLBP. Thus, BLBP is necessary (Anton et al., 1997) but not sufficient (present study) for cortical radial glia to assume their proper morphology. This might well be due to defects downstream of BLBP in the intracellular signaling in *Pax6*-deficient radial glia cells.

Our coculture experiments further suggest that *Pax6* influences radial glia cells in a cell-autonomous fashion as well as by involving cell–cell signaling. The morphological defects were not rescued in a coculture with 10× excess of cells from the wild-type cortex, supporting the notion that these defects are cell-autonomous and that *Pax6* acts directly on the morphology of cortical radial glia cells. In contrast, however, radial glia cell number was influenced by diffusible molecules. The increase of the radial glia cell number in *Pax6* loss-of-function suggests that the normal, *Pax6*-specified radial glia prevent other precursors from differentiating into radial glia cells. This scenario is strongly supported by the reduction in the number of RC2-positive mutant cortical cells to almost normal levels when cocultured with an excess of wild-type cells. Since this signaling also works through a filter membrane, diffusible molecules have to be the mediators. Indeed, diffusible molecules have been shown to induce RC2-expression in cerebellar radial glia cells (Soriano et al., 1997). Taken together, the number of radial glia cells seems to be regulated by a different mechanism than their phenotype; however, both require the function of *Pax6*.

There is thus far indirect evidence that radial glia defects might also account for phenotypic defects observed in other regions of the brain of *Pax6* mutant mice e.g., in the diencephalon. As reported previously, progenitors generated in the VZ of the third ventricle populate correctly the distinct diencephalic compartment in *Small eye* mice (Stoykova et al., 1996; Grindley et al., 1997; Warren and Price, 1997). Later, however, the progenitors in the ventral thalamus fail to differentiate in the mutant brain into nuclei and structures with proper locations and distinct expression of transcription factors *Pax6* and *Dlx1* (Stoykova et al., 1996). The processes of radial glia cells are properly orientated to serve as migratory substrates for these differentiating neurons to find their proper locations (see Edwards et al., 1990), suggesting that radial glia abnormalities might contribute to the diencephalic phenotype of the mutant brain. Similarly, the neuronal defects discovered in spinal cord of *Small eye* mutant mice (Ericson et al., 1997) might at least partially be due to alterations in the radial glia cells. It will be interesting to examine the radial glia cells in the spinal cord of *Pax6* mutants.

A similarity between spinal cord and cortical precursor cells seems to be that the precursor cells generate different cell types in the absence of functional Pax6, altered types of neurons in the spinal cord, and altered radial glia cells in cortex. Whether these alterations in cortical radial glia that are also precursor cells translates into cell fate alterations of their descendents, as in the spinal cord, remains to be determined. The transition of radial glial cells to astrocytes at the end of neurogenesis (Voigt, 1989) seems to occur normally in the cortex of *Pax6*-deficient mice as evidenced by the disappearance of the RC2 immunoreactivity at later developmental stages and the cessation of defects in cell cycle and TN-C expression. These observations suggest that at least some aspects of gliogenesis occur normally in the absence of Pax6. If radial glia cells, however, give rise to other cell types at early stages of neurogenesis (see Gray and Sanes, 1992), it will be interesting to determine whether these descendents e.g., neurons, would be affected in their phenotype in the *Pax6* mutant cortex. Also noteworthy, the *Pax6* loss-of-function in the pancreas results in a failure of generation of the glucagon-producing α cells, which normally express *Pax6* (St.-Onge et al., 1997). A unifying hypothesis might therefore be that Pax6 controls early and important steps in differentiation programs of different cell-type precursors.

Pax6 and Cell Cycle

A major feature of precursor cells is their cell cycle. We have shown here that cortical radial glia cells exhibit a higher labeling index in the absence of *Pax6* function i.e., more precursor cells are labeled by a BrdU pulse. The increased labeling index in the mutant cortex might be due to a prolongation in S phase or a shortening in cell cycle length. Since most of the regulatory events in the cell cycle take place in G1, the second scenario seems more likely.

The radial glia cells forming the hindbrain rhombomere boundaries upregulate *Pax6* correlated to a decrease in proliferation (Heyman et al., 1995), a further hint for a role of *Pax6* and cell cycle regulation. Downregulation of proliferation might be particularly important for radial glia cells, since dividing cells usually retract their processes in the M phase of the mitotic cycle, a behavior not compatible with the guidance of migrating neurons. In fact, there is some evidence that radial glia cells tightly regulate proliferation (Schmechel and Rakic, 1979a). Thus, a decrease in proliferation would help to support the guidance of migrating neurons along radial glia cell processes. This downregulation of cell division is disturbed in the absence of Pax6 in the developing cortex and might also contribute to the migrational aberrations.

Radial Glia Cells and Patterning of the Developing Brain

If *Pax6* specifies the phenotype of cortical radial glia, they should be different in some aspects from radial glia of regions devoid of *Pax6* such as the GE. We have shown here that radial glia cells from the cortex or GE exhibit different morphology in vitro. Taken together with the evidence that the influence of *Pax6* on radial glia morphology seems to be cell-autonomous, this is one of the first experimental hints for an intrinsic regional diversity of radial glia cells. Further indications of regional diversity of radial glia cells are their distinct ways of maturation. In some regions such as the cerebral cortex, they transform into multipolar astrocytes, whereas in other regions such as the cerebellum, they remain elongated and subsequently express molecules characteristic for mature astrocytes.

In the developing brain, different kinds of transient borders are established, and glial cells and glycoconjugates are their major cellular element (Steindler et al., 1990). Boundary cells delineating adjacent brain regions assume a specific phenotype. For example, radial glia fascicles have been found in rhombomere and forebrain boundaries, including the cortico-striatal border (Edwards et al., 1990; Heyman et al., 1995; Stoykova et al., 1997). As mentioned above, radial glia boundary cells between rhombomeres in the hindbrain exhibit a slower cell cycle and distinct molecular characteristics, including a specific increase in *Pax6* expression (Heyman et al., 1995). Moreover, boundaries at several locations are affected in the absence of functional Pax6 (Mastick et al., 1996; Stoykova et al., 1996, 1997; Grindley at al., 1997). This correlation prompts the suggestion that *Pax6* might contribute to the instruction of the specific phenotype of radial glia at boundaries in the developing brain.

Taken together, the role of *Pax6* in the differentiation of radial glia cells in certain regions of the developing brain provides evidence that this ubiquitous cell type is specified in a patterned manner in the developing brain.

Experimental Procedures

Animals

For this study, we used two strains of *Pax6* mutant mice: *Small eye* (*Sey* allele on a C57BL/6J $\times$ DBA/2J background), in which a point mutation in the *Pax6* results in the generation of truncated nonfunctional protein (Hill et al., 1991); and *Pax6* $-/-$ null mutants (on NMRI and C57BL/6J $\times$ DBA/2J backgrounds) produced by homologous recombination as described in St.-Onge et al. (1997). For all experiments, only littermates of homozygous and wild-type embryo brains

were compared. The day of vaginal plug was considered as E0.5. The phenotypes of the different mutants were carefully compared with regard to the aspects of the present work, and no significant differences could be detected. For example, the proportion of RC2-immunoreactive cells in acutely dissociated cells from E13.5 *Sey/Sey* was 77% (n = 422) and from *Pax6* −/− was 73% (n = 370). For most experiments, both mutants were used in parallel.

Acutely Dissociated Cells and Cultures

The lateral and medial ganglionic eminence and the cerebral cortex were isolated and prepared as described previously (Götz et al., 1996). Cells were plated at 1×10^6 per ml (0.5 ml/well) in 24-well plates onto poly-D-lysine-coated glass coverslips and cultured in defined SATO-medium (Götz et al., 1995). For some experiments, BrdU was added to the culture medium to a final concentration of 10 μM. Cells were fixed with 4% paraformaldehyde (PFA) in phosphate-buffered saline (PBS) (pH 7.4) for 15 min at room temperature.

In the coculture experiments, one cell population was labeled with the blue cell tracker dye (A2110, Molecular Probes) prior to plating as described previously (Götz et al., 1996). Unlabeled cells were plated at 0.45×10^6 per well, and 0.05×10^6–labeled cells were added. When cells were cultured on a filter insert (Millipore, 3 μm pore size), different cell densities were used that gave comparable results: 0.05×10^6 on the coverslip plus 0.45×10^6 on the filter insert or 0.5×10^6 cells on the coverslip plus 4.5×10^6 (10×) or 2×10^6 (5×) cells on the insert. Cells were fixed between 24–48 hr after plating.

Cell Lineage Analysis

BAG retrovirus was added to the primary cultures 2 hr after plating as described previously (Götz et al., 1995). Viral vectors were added at a low titre (10^4) so that no more than 20 clones per coverslip were detected after fixation. This low number of clones per coverslips reduces the probability of superimposition of two clones to 0.5% as discussed and described previously (Götz et al., 1995). For RC2 analysis, cultures were fixed after 2 days in vitro as described above, since RC2 labeling disappears after longer times (Culican et al., 1990).

Immunohistochemistry

To label cells on their day of birth, 14 mg BrdU (Sigma) per 100 g body weight was injected intraperitoneally in time-mated heterozygous *Sey* mice that were sacrificed 1 or 6 hr after the single injection (pulse labeling). Fixation and further processing were performed as described in Stoykova et al. (1997). For double immunocytochemistry, cell-type-specific antibodies were applied prior to the BrdU detection: the monoclonal antibody (mAb) RC2 (IgM; 1:60, kindly provided by P. LePrince); pAb against BLBP (kindly provided by N. Heintz); pAb against GLAST (kindly provided by M. Watanabe); mAb against β-III-tubulin (IgG2b; 1:100, Sigma); mAb against nestin (Rat 401, IgG1, 1:4, Developmental Studies Hybridoma Bank); and mAb against BrdU, IgG1, 1:10, Bioscience, Switzerland). The polyclonal antibody directed against Pax6 has been raised against a domain located between the paired and homeodomain of the Pax6 protein and was shown to recognize all known spice variants in Western blot analysis (Fritsch, 1996). It was used at a 1:1000 dilution. We also used the polyclonal Pax6 antiserum kindly given to us by R. Reed. A polyclonal antibody specific for β-galactosidase (O3G, Williams and Price, 1995) was used to detect retrovirally labeled cells (kindly provided by J. Price). Staining was performed either in cryostate sections that were fixed for 15 min in 4% PFA in PBS (pH 7.4) or in vibratome sections (100 μm thickness) that allowed better reconstruction of radial glia processes. In the latter case, brains were fixed for 6 hr in 2% PFA in PBS, then washed overnight and cut after embedding in 3% agar in PBS. Incubation in primary antisera was usually performed overnight at 4°C. Secondary rhodamine- or fluorescein-coupled antibodies were used at 1:50 (Europath) and incubated for 45 min at room temperature. After washing, slides were mounted in the glycerol-based mounting medium Poly/Mount (Polysciences) and analyzed using a Zeiss Axiophot or Biorad confocal microscope.

Apoptotic cells were detected by the TUNEL technique using the Böhringer in situ cell death detection kit.

DiI Labeling of Radial Glia Cells

The lipophilic dye DiI (Molecular probes) was applied on the pial surface of fixed brains as described previously (Voigt, 1989). DiI solution was applied onto the pial surface, where small crystals precipitated. Nonadherent crystals were washed away and the brains stored for 15 days at room temperature to allow diffusion of the dye. Brains were then embedded in 2% agar in PBS and cut frontally at a thickness of 100 μm with a vibratome. Sections were then mounted in gycerol-based mounting medium (Citifluor) and analyzed using a Zeiss Axiophot or a Biorad confocal microscope.

In Situ Hybridization

Sectioning, in situ hybridization, washing, and emulsion autoradiography were performed as previously described (Stoykova and Gruss, 1994). ^{35}S-labeled sense and anti-sense RNA probes were synthesized in the presence of two radioactive nucleotides according to the supplier's instructions (Promega) from linearized plasmid templates of TN-C (Götz et al., 1997). Two independent in situ analyses were performed for each stage on sagittal and transverse sections from wild-type and *Pax6* mutant littermate embryos. Signals were compared at corresponding levels in wild-type and *Pax6* mutant brains processed in the same in situ hybridization experiment.

Acknowledgments

We are grateful to L. St.-Onge for providing the targeted mutated *Pax6* mice. We would like to thank P. LePrince, N. Heintz, M. Watanabe, R. Reed, R. Fritsch, A. Faissner, and J. Price for kindly providing antibodies and probes. We are very grateful to E. Hartfuss for the improvement in radial glia histochemistry and to B. Grothe, J. Price, and Y. Barde for very helpful suggestions on the manuscript. We also greatly appreciate the excellent technical assistance of C. Schwarz and M. Öcalan and the photographic work of R. Altschäffel and J. Chalcroft. We thank C. Gleed and G. Goudreau for correcting the English. This work was supported by the Max-Plank-Gesellschaft and Deutsche Forschungsgemeinschaft (Leibniz award to P. G., DFG Go6402–2 to M. G.).

Received March 26, 1998; revised August 27, 1998.

References

Anton, E.S., Marchionni, M.A., Lee, K.-F., and Rakic, P. (1997). Role of GGR/neuregulin signaling in interactions between migrating neurons and radial glia in the developing cerebral cortex. Development *124*, 3501–3510.

Bartsch, S., Bartsch, U., Dörries, U., Faissner, A., Weller, A., Ekblom, P., and Schachner, M. (1992). Expression of tenascin in the developing and adult cerebellar cortex. J. Neurosci. *12*, 736–749.

Bignami, A., and Dahl, D. (1974). Astrocyte-specific protein and radial glia in the cerebral cortex of newborn rat. Nature *252*, 55–56.

Caric, D., Gooday, D., Hill, R.E., McConnell, S.K., and Price, D.J. (1997). Determination of the migratory capacity of embryonic cortical cells lacking the transcription factor *Pax-6*. Development *124*, 5087–5096.

Choi, B.H., and Lapham, L.W. (1978). Radial glia in the human fetal cerebrum: a combined Golgi, immunofluorescent and electron microscopic study. Dev. Brain Res. *148*, 295–311.

Culican, S.M., Baumrind, N.L., Yamamoto, M., and Pearlman, A.L. (1990). Cortical radial glia: Identification in tissue culture and evidence for their transformation to astrocytes. J. Neurosci. *10*, 684–692.

Edwards, M.A., Yamamoto, M., and Caviness, V.S., Jr. (1990). Organization of radial glia and related cells in the developing murine CNS. An analysis based upon a new monoclonal antibody marker. Neuroscience *36*, 121–144.

Ericson, J., Rashbass, P., Schedl, A., Brenner-Morton, S., Kawakami, A., van Heyningen, V., Jessell, T.M., and Briscoe, J. (1997). *Pax6* controls progenitor cell identity and neuronal fate in response to graded Shh signaling. Cell *90*, 169–180.

Feng, L., and Heintz, N. (1995). Differentiating neurons activate transcription of the brain lipid–binding protein gene in radial glia through a novel regulatory element. Development *121*, 1719–1730.

Feng, L., Hatten, M.E., and Heintz, N. (1994). Brain lipid–binding protein (BLBP): a novel signaling system in the developing mammalian CNS. Neuron *12*, 895–908.

Fritsch, R. (1996). The expression and function of Pax6-protein in the developing mouse. Ph.D thesis, Georg-August University, Göttingen, Federal Republic of Germany.

Gadisseux, J.-F., Kadhim, H.J., van den Bosch de Aguilar, P., Caviness, V.S., and Evrard, P. (1990). Neuronal migration within the radial glial fiber system of the developing murine cerebrum: an electron microscopic autoradiographic analysis. Dev. Brain Res. *52*, 39–56.

Götz, M., Williams, B.P., and Price, J. (1995). The specification of neuronal fate: a common precursor for neurotransmitter subtypes in the rat cerebral cortex in vitro. Eur. J. Neurosci. *7*, 889–898.

Götz, M., Wizenmann, A., Lumsden, A., and Price, J. (1996). Selective adhesion of cells from different telencephalic regions. Neuron *16*, 551–564.

Götz, M., Bolz, J., Joester, A., and Faissner, A. (1997). Tenascin-C synthesis and influence on axonal growth during rat cortical development. Eur. J. Neurosci. *9*, 496–506.

Gracheva, N.D. (1969). Autoradiography of DNA synthesis in estimation of proliferative activity of rat brain subependymal cells. Tsitologiia *11*, 1521–1527.

Gray, G.E., and Sanes, J.R. (1992). Lineage of radial glia in the chicken optic tectum. Development *114*, 271–283.

Grindley, J.C., Hargett, L.K., Hill, R.E., Ross, A., and Hogan, B.L. (1997). Disruption of *Pax6* function in mice homozygous for the *Pax6*$^{Sey\text{-}Neu}$ mutation produces abnormalities in the early development and regionalization of the diencephalon. Mech. Dev. *64*, 111–126.

Grove, E.A., Williams, B.P., Li, D.-Q., Hajihosseini, M., Friedrich, A., and Price, J. (1993). Multiple restricted lineages in the embryonic rat cerebral cortex. Development *117*, 553–561.

Halliday, A.L., and Cepko, C.L. (1992). Generation and migration of cells in the developing striatum. Neuron *9*, 15–26.

Hatten, M.E., and Mason, C.A. (1990). Mechanisms of glial-guided neuronal migration in vitro and in vivo. Experientia, *46*, 907–916.

Heyman, I., Faissner, A., and Lumsden, A. (1995). Cell and matrix specialisations of rhombomere boundaries. Dev. Dyn. *204*, 301–315.

Hill, R.E., Favor, J., Hogan, B.L.M., Ton, C.C.T., Saunders, G.F., Hanson, I.M., Prosser, J., Jordan, T., Hastie, N.D., and Van Heyningen, V. (1991). Mouse *Small eye* results from mutations in a paired-like homeobox–containing gene. Nature *354*, 522–525.

His, W. (1889). Die Neuroblasten und deren Entstehung im embryonal Marke. Abh. Math. Phys. Cl. Kgl. Sach. Ges. Wiss. *15*, 313–372.

Hockfield, S., and McKay, R.D. (1985). Identification of major cell classes in the developing mammalian nervous system. J. Neurosci. *5*, 3310–3328.

Hunter, K.E., and Hatten, M.E. (1995). Radial glial cell transformation to astrocytes is bidirectional: regulation by a diffusible factor in embryonic forebrain. PNAS *92*, 2061–2065.

Kurtz, A., Zimmer, A., Schnütgen, F., Brüning, G., Spener, F., and Müller, T. (1994). The expression pattern of a novel gene encoding brain–fatty acid binding protein correlated with neuronal and glial development. Development *120*, 2637–2649.

Levitt, P., Cooper, M.L., and Rakic, P. (1981). Coexistence of neuronal and glial precursor cells in the cerebral ventricular zone of the fetal monkey: an ultrastructural immunoperoxidase analysis. J. Neurosci. *1*, 27–39.

Levitt, P., Cooper, M.L., and Rakic, P. (1983). Early divergence and changing proportions of neuronal and glial precursor cells in the primate cerebral ventricular zone. Dev. Biol. *96*, 472–484.

Luskin, M.B., Parnavelas, J.G., and Barfield, J.A. (1993). Neurons, astrocytes and oligodendrocytes of the rat cerebral cortex originate from separate progenitor cells: an ultrastructural analysis of clonally related cells. J. Neurosci. *13*, 1730–1750.

Mastick, G.S., Davis, N.M., Andrew, G.L., and Easter, S.S., Jr. (1996). *Pax-6* functions in boundary formation and axon guidance in the embryonic mouse forebrain. Development *124*, 1985–1997.

Misson, J.-P., Edwards, M.A., Yamamoto, M., and Caviness, V.S., Jr. (1988). Identification of radial glial cells within the developing murine central nervous system: Studies based upon a new immunohistochemical marker. Dev. Brain Res. *44*, 95–108.

Misson, J.-P., Takahashi, T., and Caviness, V.S., Jr. (1991). Ontogeny of radial and other astroglial cells in murine cerebral cortex. Glia 4, 138–148.

Mitrovic, N., Dörries, U., and Schachner, M. (1994). Expression of the extracellular matrix glycoprotein tenascin in the somatosensory cortex of the mouse during postnatal development: an immunocytochemical and in situ hybridization analysis. J. Neurocytol. *23*, 364–378.

Pinto-Lord, M.C., Evrard, P., and Caviness, V.S., Jr. (1982). Obstructed neuronal migration along radial glia fibers in the neocortex of the *reeler* mouse: a Golgi-EM analysis. Dev. Brain Res. *4*, 379–393.

Pixley, S.K.R., and DeVellis, J. (1984). Transition between immature radial glia and mature astrocytes studied with a monoclonal antibody to vimentin. Dev. Brain Res. *15*, 201–209.

Rakic, P. (1972). Mode of cell migration to the superficial layers of fetal monkey neocortex. J. Comp. Neurol. *145*, 61–84.

Rakic, P., Cameron, R.S., and Komuro, H. (1994). Recognition, adhesion, transmembrane signaling and cell motility in guided neuronal migration. Curr. Opin. Neurobiol. *4*, 63–69.

Ramón y Cajal, S. (1890). Sur l'origine et les ramifications des fibres nerveuses de la moelle embryonnaire. Anat. Anz. *5*, 85–95, 111–119.

Reid, C.B., Liang, I., and Walsh, C. (1995). Systematic widespread clonal organization in the cerebral cortex. Neuron *15*, 299–310.

Sauer, F.C. (1935). Mitosis in the neural tube. J. Comp. Neurol. *62*, 377–405.

Schmahl, W., Knoedlseder, M., Favor, J., and Davidson, D. (1993). Defects of neuronal migration and the pathogenesis of cortical malformations are associated with *Small Eye* (*Sey*) in the mouse, a point mutation at the *Pax6*-locus. Acta Neuropathol. *86*, 126–135.

Schmechel, D.E., and Rakic, P. (1979a). Arrested proliferation of radial glia cells during midgestation in rhesus monkey. Nature *277*, 303–305.

Schmechel, D.E., and Rakic, P. (1979b). A Golgi study of rat glial cells in developing monkey telencephalon: morphogenesis and transformation into astrocytes. Anat. Embryol. (Berl) *156*, 115–152.

Shibata, T., Yamada, K., Watanabe, M., Ikenaka, K., Wada, K., Tanaka, K., and Inoue, Y. (1997). Glutamate transporter GLAST is expressed in the radial glia-astrocyte lineage of developing mouse spinal cord. J. Neurosci. *17*, 9212–9219.

Soriano, E., Alvarado-Mallart, R.-M., Dumesnil, N., Del Rio, J., and Sotelo, C. (1997). Cajal-Retzius cells regulate the radial glia phenotype in the adult and developing cerebellum and alter granule cell migration. Neuron *18*, 563–577.

St.-Onge, L., Sosa-Pineda, B., Chowdhury, K., Mansouri, A., and Gruss, P. (1997). Pax6 is required for differentiation of glucagon-producing alpha-cells in mouse pancreas. Nature *387*, 406–409.

Steindler, D.A., O'Brien, T.F., Laywell, E., Harrington, K., Faissner, A., and Schachner, M., (1990). Boundaries during normal and abnormal brain development: in vivo and in vitro studies of glia and glycoconjugates. Exp. Neurol. *109*, 35–56.

Stoykova, A., and Gruss, P. (1994). Roles of *Pax*-genes in developing and adult brain as suggested by expression patterns. J. Neurosci. *14*, 1395–1412.

Stoykova, A., Fritsch, R., Walther, C., and Gruss, P. (1996). Forebrain patterning defects in *Small eye* mutant mice. Development *122*, 3453–3465.

Stoykova, A., Götz, M., Gruss, P., and Price, J. (1997). *Pax6*-dependent regulation of adhesive patterning, R-cadherin expression and boundary formation in the developing forebrain. Development *124*, 3765–3777.

Voigt, T. (1989). Development of glial cells in the cerebral wall of ferrets: direct tracing of their transformation from radial glia into astrocytes. J. Comp. Neurol. *289*, 74–88.

Walther, C., and Gruss, P. (1991). *Pax-6*, a murine paired-box gene, is expressed in the developing CNS. Development *113*, 1435–1449.

Williams, B.P., and Price, J. (1995). Evidence for multiple precursor cell types in the embryonic rat cerebral cortex. Neuron *14*, 1181–1188.

Warren, N., and Price, D.J. (1997). Roles of *Pax-6* in murine diencephalic development. Development *124*, 1573–1582.